Anisotropic Two-Dimensional Disordered Wigner Solid

Md. S. Hossain, M. K. Ma, K. A. Villegas-Rosales, Y. J. Chung, L. N. Pfeiffer, K. W. West, K. W. Baldwin, and M. Shayegan

Phys. Rev. Lett. **129**, 036601 — Published 13 July 2022

DOI: 10.1103/PhysRevLett.129.036601

Anisotropic, two-dimensional, disordered Wigner solid

Md. S. Hossain, M. K. Ma, K. A. Villegas-Rosales, Y. J. Chung, L. N. Pfeiffer, K. W. West, K. W. Baldwin, and M. Shayegan
Department of Electrical Engineering, Princeton University, Princeton, New Jersey 08544, USA
(Dated: June 7, 2022)

The interplay between the Fermi sea anisotropy, electron-electron interaction, and localization phenomena can give rise to exotic many-body phases. An exciting example is an *anisotropic* two-dimensional (2D) Wigner solid (WS), where electrons form an ordered array with an anisotropic lattice structure. Such a state has eluded experiments up to now as its realization is extremely demanding: First, a WS entails very low densities where the Coulomb interaction dominates over the kinetic (Fermi) energy. Attaining such low densities while keeping the disorder low is very challenging. Second, the low-density requirement has to be fulfilled in a material that hosts an anisotropic Fermi sea. Here, we report transport measurements in a clean (low-disorder) 2D electron system with anisotropic effective mass and Fermi sea. The data reveal that at extremely low electron densities, when the r_s parameter, the ratio of the Coulomb to the Fermi energy, exceeds $\simeq 38$, the current-voltage characteristics become strongly nonlinear at small DC biases. Several key features of the nonlinear characteristics, including their anisotropic voltage thresholds, are consistent with the formation of a disordered, anisotropic WS pinned by the ubiquitous disorder potential.

Strong electron-electron interaction in clean two-dimensional electron systems (2DESs) leads to a plethora of many-body phases such as fractional quantum Hall liquid [1], Wigner solid (WS) [2–21], and correlated magnetism [16, 22–29]. Anisotropy introduces a new flavor to the interaction phenomena and triggers yet another set of unexpected correlated phases [30–43], such as nematic quantum Hall states [32, 34–36, 40, 42]. A tantalizing example of Fermi sea anisotropy induced many-body states is a theoretically proposed anisotropic WS at zero magnetic field [30]. This state is predicted to emerge at very low densities, harboring antiferromagnetic order [31]. However, such a state at zero magnetic field has eluded experiments [44] because of the absence of a clean material platform where the low-density electrons occupy an anisotropic Fermi sea.

Realization of a WS by itself is challenging. It requires Coulomb interaction (E_C) to dominate over the thermal energy (k_BT) and Fermi energy (E_F) [2]. In a system where $E_F >> k_BT$ a *quantum* WS should form when E_C far exceeds E_F. This criterion can be realized at very low electron densities. Quantitatively, in an ideal 2DES, Monte Carlo calculations [23–25] indicate that electrons should freeze into a quantum WS when the parameter r_s exceeds $\simeq 35$; r_s is the average inter-electron distance in units of the effective Bohr radius, equivalently, $r_s = E_C/E_F$. Achieving such large r_s values and a sufficiently clean 2DES so that interaction phenomena are not completely hindered by excessive disorder and single-particle localization, however, is extremely challenging. Note that for a 2DES, $r_s = (m^*e^2/4\pi\hbar^2\varepsilon\varepsilon_0)/(\pi n)^{1/2}$, where m^* is the electron band effective mass, ε is the dielectric constant, and n is the 2DES density. In a GaAs 2DES ($m^* = 0.067m_e$, where m_e is the free electron mas and $\varepsilon = 13$), $r_s \simeq 35$ corresponds to a density of $n = 2.5 \times 10^8$ cm^{-2}, which is indeed very difficult to attain [45, 46]. In systems with a larger m^*, high r_s can be obtained at reasonable densities [10, 16, 19–21]. In fact, there are reports of a WS formation in GaAs 2D *holes* [10], and AlAs [16], $MoSe_2$ [19, 20], and ZnO [21] electrons. Here we attain extremely low densities and very large r_s (up to $\simeq 50$) in an *anisotropic* system and reveal an intriguing interplay between anisotropy and many-body localization in the WS regime.

Our material platform is a high-quality 2DES confined to a 21-nm-wide AlAs quantum well [47–51]. The 2D electrons in the AlAs well occupy two in-plane conduction-band valleys with longitudinal and transverse effective masses $m_l = 1.1$, and $m_t = 0.20$, leading to an effective in-plane $m^* = (m_lm_t)^{1/2} = 0.46$ [47–51]. Via applying uniaxial strain along the [100] direction we transfer all the electrons to the valley whose longer Fermi wavevector axis is along the [010] direction [47]; we refer to this as the Y valley, see Fig. 1(a). As discussed below, this single-valley occupancy can also be achieved, in the absence of uniaxial strain, by tuning n to very small values; n is controlled *in situ* by applying voltage to a back gate. The exceptionally high quality of our 2DES can be inferred from Fig. 1(b) which shows magnetoresistance traces measured along [100] as a function of the perpendicular magnetic field (B) for several n ranging from 2.82 to 1.00, in units of 10^{10} cm^{-2} which we use throughout this paper. We plot the data as a function of ν^{-1} so that the quantum Hall states line up for the different traces; $\nu = nh/eB$ is the Landau level filling factor. The traces exhibit clear minima at $\nu = 1/3$ down to $n = 1.20$ ($r_s = 44.6$ [57]), indicating the presence of fractional quantum Hall states and attesting to the very high sample quality.

Figure 1(c), which presents the sample resistance along [100] and [010], provides an overview of the different transitions and phases observed in our sample as n is lowered. Here there is no uniaxial strain applied so that the two in-plane valleys (X and Y), with their major axes along [100] and [010], are equally occupied at high densities; $R_{[100]}$ and $R_{[010]}$ are essentially equal and the 2DES is isotropic. As n is lowered below $\simeq 6.3$ ($r_s \simeq 20$), all the electrons suddenly transfer to the Y valley, leading to $R_{[010]} > R_{[100]}$ (note that the electrons in the Y valley have a larger effective mass along [010] compared to [100]). This abrupt, spontaneous valley-

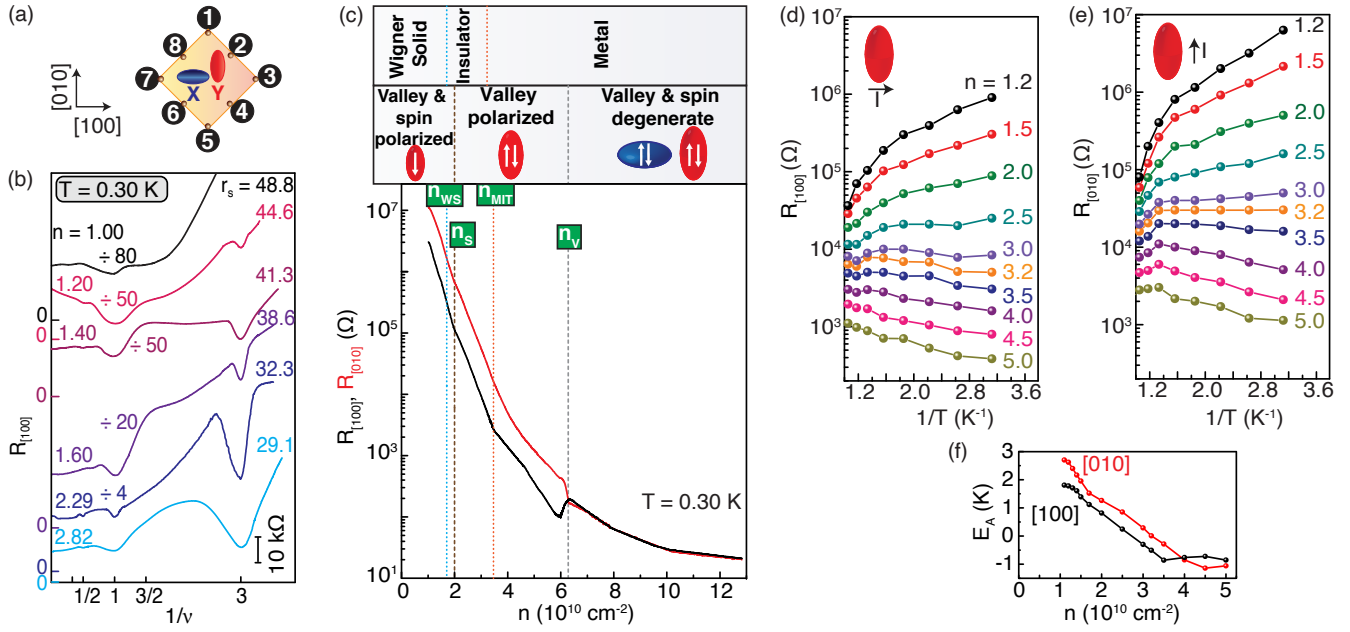

FIG. 1. Overview of our sample's geometry and its transport data. (a) Top view of our sample, an AlAs quantum well, in which the 2D electrons can occupy one or two anisotropic conduction-band valleys. Projections of the anisotropic Fermi seas of the X and Y valleys are shown in blue and red; these valleys have their major axes along the [100] and [010] crystallographic directions, respectively. The sample has a $\simeq 1.5 \times 1.5$ mm^2 van der Pauw geometry, and contacts to the sample are denoted by 1-8. For measuring $R_{[100]}$, we pass current from contact 8 to 2 and measure the voltage between contacts 6 and 4. For $R_{[010]}$, the current is passed from contact 8 to 6 and we measure the voltage between contacts 2 and 4. (b) Magnetoresistance traces taken along [100] as a function of the perpendicular magnetic field at different densities n, as indicated (in units of 10^{10} cm^{-2}), highlighting the extremely high quality of the 2DES at very low densities and large r_s. Traces are shifted vertically, and are plotted vs. $1/\nu$. In all these traces, all the 2D electrons occupy the Y valley. (c) Resistances along [100] and [010] directions at zero strain as a function of density. $R_{[100]}$ and $R_{[010]}$ suddenly split when a spontaneous valley transition occurs at $n_V \simeq 6.3$. Also, two clear "kinks (marked with vertical lines) are seen at $n \simeq 3.5$ and 2.0 which closely correlate with the onset of the metal-insulator transition (n_{MIT}) and the spontaneous spin transition, respectively. At even lower densities, below $n_{WS} \simeq 1.80$, we start to see non-linear I-V characteristics, suggestive of a pinned WS; this is the main subject of our work presented here. (d,e) Arrhenius plots of $R_{[100]}$ and $R_{[010]}$. Both $R_{[100]}$ and $R_{[010]}$ exhibit metallic transport for $n \gtrsim 3$, and an insulating behavior for smaller n. $R_{[100]}$ and $R_{[010]}$ exhibit approximately an activated behavior at low T ($\lesssim 0.6$ K), $R \propto e^{E_A/2k_BT}$, for $n \lesssim 3$. (f) shows the deduced E_A along [100] and [010] vs. density.

polarization, which is akin to Bloch spin ferromagnetism transition, has been discussed in detail elsewhere [43]; see also [58]. At lower densities, when $n \lesssim 3.2$ ($r_s \gtrsim 28$), the 2DES turns insulating as signaled by the temperature dependence of $R_{[100]}$ and $R_{[010]}$ at low temperatures; see Figs. 1(d,e). Note in Fig. 2(d) that near this transition to an insulating phase, we observe a "kink" in resistance vs. n traces. At even lower densities, $n \lesssim 2.0$ ($r_s \gtrsim 35$), the 2DES makes yet another transition to a fully-spin-polarized state [16]. Finally, at $n \lesssim 1.8$ ($r_s \gtrsim 37$), the 2DES becomes highly insulating while still maintaining its anisotropic transport coefficients, and develops a strongly nonlinear *I-V* characteristic at low temperatures [59]. This phase is the focus of our report here.

The highlight of our study is presented in Fig. 2(a) where we show the differential resistance dV/dI along [100] and [010] vs. the DC bias voltage (V_{DC}) at very low densities. For Fig. 2 data, as well as in Fig. 3, the 2D electrons occupy only the Y valley. We use log-log plots to cover several orders of magnitude in dV/dI and V_{DC}. The data in Fig. 2(a) show nonlinear I-V behavior, with clear threshold voltages (V_{th}) that are larger along [010] compared to [100] (for a given density) [60]. We attribute these nonlinearities to the formation of a WS pinned by the ubiquitous disorder potential. Similar nonlinearities at small biases have been observed in previous studies of dilute GaAs 2D holes at $B = 0$ [10], and at very small Landau level fillings in the extreme quantum limit [5, 6], which also concluded that the nonlinearity in I-V was a signature of the depinning of a WS. The conclusion for high-B data has been further corroborated by numerous experimental studies at very small Landau level fillings, including transport [4], noise [6], magneto-optics [7], microwave [3, 11], nuclear magnetic resonance [12], tunneling [14], geometric resonance [13], and capacitance [15] measurements. Therefore, it is likely that in our 2DES, too, the nonlinear *I-V* signals the formation of a pinned WS at $r_s \gtrsim 37$ ($n \lesssim 1.80$). Below we elaborate on several important features of the nonlinearities in Fig. 2(a), and argue that they are consistent with an interpretation of our data in terms of a disordered, *anisotropic* WS.

A key observation in our data is that the magnitude of the threshold electric field (E_{th}) is consistent with the expected depinning of a 2D WS [10]. For example, Chui [61] proposed

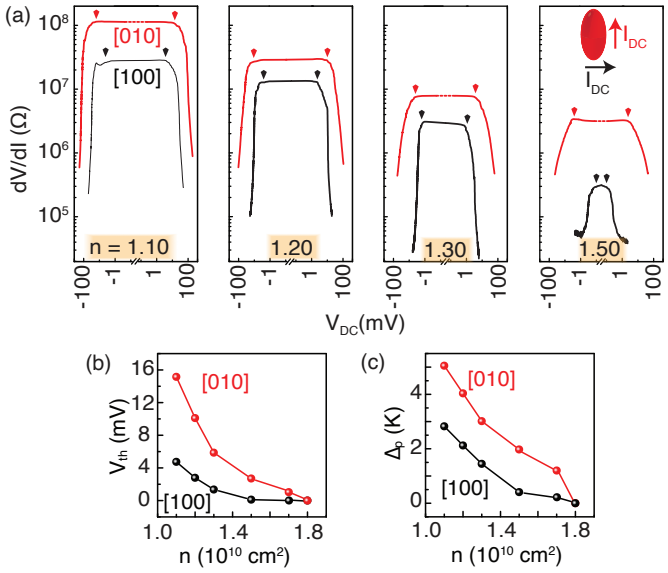

FIG. 2. (a) dV/dI data at $T = 0.30$ K along the [100] (black traces) and [010] (red traces) crystallographic directions, plotted as a function of the DC voltage drop along the sample; data are shown for $n = 1.10$, 1.20, 1.30, and 1.50 (in units of 10^{10} cm^{-2}). Along both directions dV/dI traces show a reasonably abrupt drop above a threshold voltage (V_{th}). The vertical arrows (placed symmetrically with respect to $V_{DC} = 0$) mark V_{th}, and are based on the average value of V_{th} for $+V_{DC}$ and $-V_{DC}$. (b) Extracted V_{th} and (c) pinning gap (Δ_p) plotted vs. n, highlighting the increase in V_{th} and Δ_p as n is lowered.

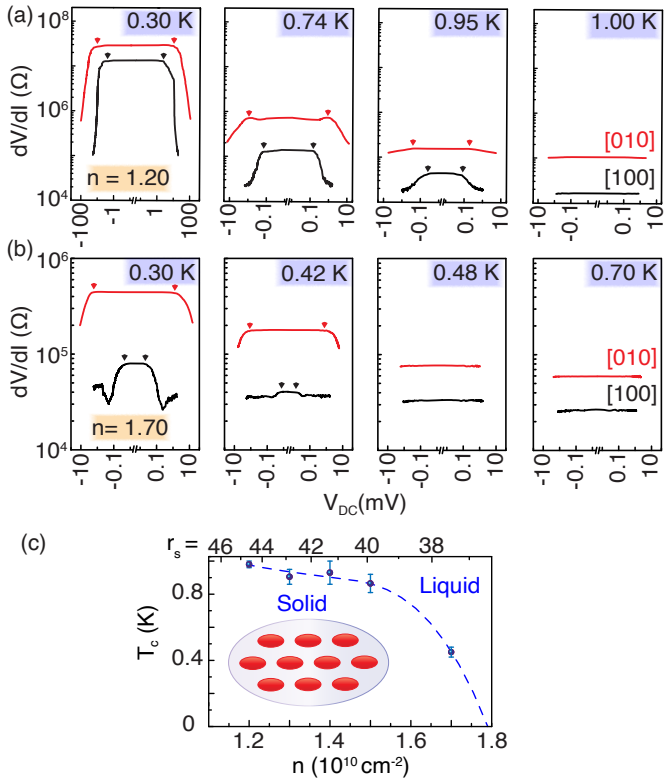

FIG. 3. Temperature dependence of dV/dI vs. V_{DC} at (a) $n = 1.20$ and (b) $n = 1.70$, measured along [100] and [010] directions. (c) Critical temperature (T_c), below which the I-V characteristic becomes nonlinear, plotted vs. electron density. The data suggest a drop in T_c with increasing density, extrapolating to 0 K as the onset density for the pinned WS formation ($n \simeq 1.80$) is reached. The dashed curve is a guide to the eye. The inset displays schematically an anisotropic WS; the shaded regions represent the electron charge distribution with anisotropic Bohr radii, reflecting the anisotropic electron effective mass.

a model in which the WS is weakly pinned by the potential of the remote ionized dopants, and transport takes place through the creation of dislocation pairs and quantum tunneling. In this model, it is estimated that:

$$E_{th} \simeq 0.09 n_i a^2 e/(4\pi\varepsilon d^3), \qquad (1)$$

where n_i is the density of remote ionized impurities, $a = (\pi n)^{-1/2}$, and d is the spacer-layer thickness. Using relevant and reasonable parameters for our sample ($\varepsilon = 10$, $d = 68$ nm, $n = 1.3$, and $n_i = 2 \times 10^{11}$ cm^{-2} [62]), we estimate $E_{th} \simeq 5$ V/m. Given that the distance between voltage contacts in our sample [e.g., contacts 2 and 8 in Fig. 1(a)] is $\simeq 1$ mm, $E_{th} \simeq 5$ V/m corresponds to $V_{th} \simeq 5$ mV; this is of the order of V_{th} we observe in our experiments [see Fig. 2(b)]. Given the uncertainty in the value of n_i, we believe our data are consistent with the model of Ref. [61] for a pinned WS.

A related implication of Fig. 2 data is the WC pinning energy $\Delta_p \simeq \hbar(eE_{th}/m^*a)^{1/2}$ that can be deduced from the measured V_{th} [10]. In Fig. 2(c) we plot, as a function of n, the values of Δ_p deduced from the V_{th} data of Fig. 2(b). Note that Eq. (1) and the above expression for Δ_p imply that both V_{th} and Δ_p should increase as the density is lowered. This behavior is seen qualitatively in Figs. 2(b,c). Moreover, the magnitude of Δ_p should be comparable to the activation energies extracted from the Arrhenius plots in Fig. 1(f), and this is indeed true, as both sets of data yield energies of a few K.

The V_{th} data can be used to also extract an approximate size for the WS domain: $L_0^2 = 0.02e/4\pi\varepsilon\varepsilon_0 E_{th}$ [6]. This expression is based on a theory by Fukuyama and Lee [63], and uses the 2D WS shear modulus calculated by Bonsall and Maradudin [64]. Evaluating this expression for our data at $n = 1.3$, where $E_{th} \sim 4$ V/m [see Fig. 2(b)], we find $L_0^2 \sim 7 \times 10^{-13}$ m^2, implying that a typical WS domain contains $nL_0^2 \sim 90$ electrons. This is admittedly not a very large domain, but is plausible, given the amount of disorder in our sample. Note also that, in this model, the anisotropy of E_{th} implies that the WS domains are anisotropic too, with the domain size along [010] being larger than along [100].

Data of Fig. 3 illustrate another aspect of our 2DES. In Figs. 3(a,b) we show the temperature dependence of nonlinear dV/dI along [100] and [010] at two different densities, $n = 1.20$ and 1.70. The data indicate that, for a given n and direction, V_{th} moves to smaller values as T is raised, and the nonlinearity disappears above a critical temperature T_c. We interpret this disappearance to signal the thermal melting of the WS. As seen in Fig. 3(a), T_c at $n = 1.20$ appears to be

between 0.95 K and 1.00 K. Note that the data along [100] and [010] exhibit a similar temperature dependence, implying the same T_c along both directions. When we raise the density, T_c decreases. For example, at $n = 1.70$, the nonlinearity disappears for $T \gtrsim 0.48$ K [Fig. 3(b)]. Figure 3(c) summarizes the measured T_c as a function of n. As we raise the density, up to $n = 1.50$, T_c decreases only slightly. However, T_c drops rapidly at higher n, implying a quantum melting of the WS at $n \simeq 1.80$.

The critical temperatures we summarize in Fig. 3(c) are about an order of magnitude larger than the melting temperatures theoretically estimated for an ideal (zero-disorder) quantum WS with parameters similar to our 2DES [see, e.g. Fig. 2(a) of Ref. [65] for GaAs 2D holes]. Also, in our sample the Fermi energy at the lowest densities is small and becomes comparable to the measurement temperatures; this implies that our 2DES approaches the classical limit. It is likely that pinning by the impurities at very low densities is what leads to the much larger melting temperatures in our sample. Indeed, recent theoretical studies, partly motivated by our results, indicate that the effective melting temperature of a WS in the presence of disorder can be significantly enhanced relative to the pristine case as the disordered WS becomes fragmented and localized by the disorder potential [66, 67]. Moreover, in a system with disorder, the 2DES eventually attains an Anderson localized state in the limit of extremely small densities because the disorder potential would dominate over the ever-decreasing Coulomb repulsion energy. We note that T_c in Fig. 3(c) are comparable to the melting temperatures reported for the magnetic-field-induced WS phases of dilute 2DESs in GaAs [5, 11, 15] and AlAs [18], and 2D holes in GaAs [17]. They are much smaller than those recently quoted for the zero-field WS phases in $MoSe_2$ [19, 20], but much larger than in ZnO [21].

We close by making several comments concerning the anisotropy observed in our data. First, Fig. 1(b) data show that the transport anisotropy persists in the entire low-density range once all the electrons are transferred to the Y valley (below $n = 6.3$). This includes the high densities (e.g., $n \simeq 4$), when the 2DES is in a "metallic" state, and also deep into the insulating phases at very low densities. Second, V_{th} for the onset of drops in dV/dI vs. V_{DC} also show an anisotropy, with V_{th} along [010] being larger compared to [100] (Figs. 2 and 3). These features are very likely related to the anisotropic effective mass in our 2DES. For a 2DES like ours, with a large effective mass along the y direction ($m_l = 1.1$) and a small mass along x ($m_t = 0.20$), the electron charge distribution has an elliptical shape which is rotated by 90^o with respect to the shape of the Fermi sea/contour [see Fig. 3(c) inset]. Such a charge distribution would imply that transport along y would be harder compared to x as the electrons are more localized (smaller Bohr radius) and have less overlap along y. This is consistent with our observations. Now, theory [30] suggests that in a 2DES with an anisotropic effective mass, the WS is distorted from its conventional, triangular lattice, and has a shape schematically shown in Fig. 3(c) inset. Note that, compared to the conventional triangular lattice, here the lattice is stretched along the x axis. (The stretch along the axis of the smaller mass reduces the longitudinal energy of lattice vibrations, thus lowering the ground state energy [30]). It then appears that the transport and V_{th} anisotropies would depend on the competition between the anisotropies of the electron charge distribution and the WS lattice, e.g., a very large elongation of the lattice might eventually lead to a reversal of the transport anisotropy, with resistance and V_{th} along x exceeding those along y. We do not observe such reversal of anisotropies, suggesting that the transport anisotropy in our 2DES is controlled by the electron charge distribution anisotropy.

We acknowledge support through the U.S. Department of Energy Basic Energy Sciences (Grant No. DEFG02-00-ER45841) for measurements, and the National Science Foundation (Grants No. DMR 2104771, No. ECCS 1906253, DMR 1709076, and MRSEC DMR 2011750), the Eric and Wendy Schmidt Transformative Technology Fund, and the Gordon and Betty Moore Foundations EPiQS Initiative (Grant No. GBMF9615 to L. N. P.) for sample fabrication and characterization. We also thank J. K. Jain, S. Das Sarma, L. W. Engel, D. A. Huse, M. A. Mueed, and B. Shklovskii for illuminating discussions.

[1] D. C. Tsui, H. L. Stormer, and A. C. Gossard, Two-dimensional magnetotransport in the extreme quantum limit, Phys. Rev. Lett. **48**, 1559 (1982).
[2] E. Wigner, On the interaction of electrons in metals, Phys. Rev. **46**, 1002 (1934).
[3] E. Y. Andrei, G. Deville, D. C. Glattli, F. I. B. Williams, E. Paris, and B. Etienne, Observation of a Magnetically Induced Wigner Solid, Phys. Rev. Lett. **60**, 2765 (1988).
[4] H. W. Jiang, R. L. Willett, H. L. Stormer, D. C. Tsui, L. N. Pfeiffer, and K. W. West, Quantum liquid versus electron solid around $\nu = 1/5$ Landau-level filling, Phys. Rev. Lett. **65**, 633 (1990).
[5] V. J. Goldman, M. Santos, M. Shayegan, and J. E. Cunningham, Evidence for two-dimentional quantum Wigner crystal, Phys. Rev. Lett. **65**, 2189 (1990).
[6] Y. P. Li, T. Sajoto, L. W. Engel, D. C. Tsui, and M. Shayegan, M. Low-frequency noise in the reentrant insulating phase around the $1/5$ fractional quantum Hall liquid, Phys. Rev. Lett. **67**, 1630 (1991).
[7] H. Buhmann, W. Joss, K. von Klitzing, I. V. Kukushkin, A. S. Plaut, G. Martinez, K. Ploog, and V. B. Timofeev, Novel magneto-optical behavior in the Wigner-solid regime, Phys. Rev. Lett. **66**, 926 (1991).
[8] M. B. Santos, Y. W. Suen, M. Shayegan, Y. P. Li, L. W. Engel, and D. C. Tsui, Observation of a reentrant insulating phase near the 1/3 fractional quantum Hall liquid in a two-dimensional hole system, Phys. Rev. Lett. **68**, 1188 (1992).
[9] M. B. Santos, J. Jo, Y. W. Suen, L. W. Engel, and M. Shayegan, Effect of Landau-level mixing on quantum-liquid and solid states of two-dimensional hole systems, Phys. Rev. B **46**, 13639(R) (1992).
[10] J. Yoon, C. C. Li, D. Shahar, D. C. Tsui, and M. Shayegan,

Wigner Crystallization and Metal-Insulator Transition of Two-Dimensional Holes in GaAs at $B = 0$, Phys. Rev. Lett. **82**, 1744 (1999).

[11] Y. P. Chen, G. Sambandamurthy, Z. H. Wang, R. M. Lewis, L. W. Engel, D. C. Tsui, P. D. Ye, L. N. Pfeiffer, and K. W. West, Melting of a 2D quantum electron solid in high magnetic field, Nat. Phys. **2**, 452 (2006).

[12] L. Tiemann, T. D. Rhone, N. Shibata, and K. Muraki, NMR profiling of quantum electron solids in high magnetic fields, Nat. Phys. **10**, 648 (2014).

[13] H. Deng, Y. Liu, I. Jo, L. N. Pfeiffer, K. W. West, K. W. Baldwin, and M. Shayegan, Commensurability Oscillations of Composite Fermions Induced by the Periodic Potential of a Wigner Crystal,Phys. Rev. Lett. **117**, 096601 (2016).

[14] J. Jang, B. M. Hunt, L. N. Pfeiffer, K. W. West, and R. C. Ashoori, Sharp tunnelling resonance from the vibrations of an electronic Wigner crystal, Nat. Phys. **13**, 340 (2017).

[15] H. Deng, L. N. Pfeiffer, K. W. West, K. W. Baldwin, L. W. Engel, and M. Shayegan, Probing the Melting of a Two-Dimensional Quantum Wigner Crystal via its Screening Efficiency, Phys. Rev. Lett. **122**, 116601 (2019).

[16] M. S. Hossain, M. K. Ma, K. A. Villegas Rosales, Y. J. Chung, L. N. Pfeiffer, K. W. West, K. W. Baldwin, and M. Shayegan, Observation of spontaneous ferromagnetism in a two-dimensional electron system, Proc. National Acad. Sci. **117**, 32244 (2020).

[17] M. K. Ma, K. A. Villegas Rosales, H. Deng, Y. J. Chung, L. N. Pfeiffer, K. W. West, K. W. Baldwin, R. Winkler, and M. Shayegan, Thermal and Quantum Melting Phase Diagrams for a Magnetic-Field-Induced Wigner Solid, Phys. Rev. Lett. **125**, 036601 (2020).

[18] K. A. Villegas Rosales, S. K. Singh, Meng K. Ma, Md. Shafayat Hossain, Y. J. Chung, L. N. Pfeiffer, K. W. West, K. W. Baldwin, and M. Shayegan, Competition between fractional quantum Hall liquid and Wigner solid at small fillings: Role of layer thickness and Landau level mixing, Phys. Rev. Research **3**, 013181 (2021).

[19] Y. Zhou, J. Sung, E. Brutschea, I. Esterlis, Y. Wang, G. Scuri, R. J. Gelly, H. Heo, T. Taniguchi, K. Watanabe, G. Zaránd, M. D. Lukin, P. Kim, E. Demler, and H. Park, Bilayer Wigner crystals in a transition metal dichalcogenide heterostructure, Nature **595**, 48 (2021).

[20] T. Smoleński, P. E. Dolgirev, C. Kuhlenkamp, A. Popert, Y. Shimazaki, P. Back, X. Lu, M. Kroner, Kenji Watanabe, T. Taniguchi, I. Esterlis, E. Demler, and Ataç Imamoğlu, Signatures of Wigner crystal of electrons in a monolayer semiconductor, Nature **595**, 53 (2021)

[21] J. Falson, I. Sodemann, B. Skinner, D. Tabrea, Y. Kozuka, A. Tsukazaki, M. Kawasaki, K. von Klitzing, and J. H. Smet, Competing correlated states around the zero field Wigner crystallization transition of electrons in two-dimensions, Nature Materials **21**, 311 (2022).

[22] F. Bloch, Bemerkung zur Elektronentheorie des Ferromagnetismus und der elektrischen Leitfähigkeit, Z. Phys. **57**, 545 (1929).

[23] B. Tanatar and D. M. Ceperley, Ground state of the two-dimensional electron gas, Phys. Rev. B **39**, 5005 (1989).

[24] C. Attaccalite, S. Moroni, P. Gori-Giorgi, and G. B. Bachelet, Correlation energy and spin polarization in the 2D electron gas, Phys. Rev. Lett. **88**, 256601 (2002).

[25] N. D. Drummond and R. J. Needs, Phase Diagram of the Low-Density Two-Dimensional Homogeneous Electron Gas, Phys. Rev. Lett. **102**, 126402 (2009).

[26] A. L. Sharpe, E. J. Fox, A. W. Barnard, , J. Finney, K.Watanabe, T. Taniguchi, M. A. Kastner, and D. Goldhaber-Gordon, Emergent ferromagnetism near three-quarters filling in twisted bilayer graphene, Science **365**, 605 (2019).

[27] J. G. Roch, D. Miserev, G. Froehlicher, N. Leisgang, L. Sponfeldner, K. Watanabe, T. Taniguchi, J. Klinovaja, Daniel Loss, and Richard J. Warburton, First-Order Magnetic Phase Transition of Mobile Electrons in Monolayer MoS_2, Phys. Rev. Lett. **124**, 187602 (2020).

[28] H. Polshyn, J. Zhu, M. A. Kumar, Y. Zhang, F. Yang, C. L. Tschirhart, M. Serlin, K. Watanabe, T. Taniguchi, A. H. MacDonald, and A. F. Young, Electrical switching of magnetic order in an orbital Chern insulator, Nature **588**, 66 (2020).

[29] Md. S. Hossain, T. Zhao, S. Pu, M. A. Mueed, M. K. Ma, K. A. V. Rosales, Y. J. Chung, L. N. Pfeiffer, K. W. West, K. W. Baldwin, J. K. Jain, M. Shayegan, Bloch ferromagnetism of composite fermions, Nat. Phys. **17**, 48 (2021) (2021).

[30] X. Wan and R. N. Bhatt, Two-dimensional Wigner crystal in anisotropic semiconductors, Phys. Rev. B **65**, 233209 (2002).

[31] C. Zhou and R. N. Bhatt, Zero temperature magnetic phase diagram of Wigner crystal in anisotropic two-dimensional electron systems, Physica B: Condensed Matter **403**, 1547 (2008).

[32] J. Xia, J. P. Eisenstein, L. N. Pfeiffer, and K. W. West, Evidence for a fractionally quantized Hall state with anisotropic longitudinal transport, Nat. Phys. **7**, 845 (2011).

[33] T. Gokmen, M. Padmanabhan, and M. Shayegan, Transference of transport anisotropy to composite fermions, Nat. Phys. **6**, 621 (2010).

[34] M. Mulligan, C. Nayak, and S. Kachru, Effective field theory of fractional quantized Hall nematics, Phys. Rev. B **84**, 195124 (2011).

[35] B. Yang, Z. Papić, E. H. Rezayi, R. N. Bhatt, and F. D. M. Haldane, Band mass anisotropy and the intrinsic metric of fractional quantum Hall systems, Phys. Rev. B **85**, 165318 (2012).

[36] Y. Liu, S. Hasdemir, M. Shayegan, L. N. Pfeiffer, K. W. West, and K. W. Baldwin, Evidence for a $\nu = 5/2$ fractional quantum Hall nematic state in parallel magnetic fields, Phys. Rev. B **88**, 035307 (2013).

[37] D. Kamburov, Yang Liu, M. Shayegan, L. N. Pfeiffer, K. W. West, and K. W. Baldwin, Composite Fermions with Tunable Fermi Contour Anisotropy, Phys. Rev. Lett. **110**, 206801 (2013).

[38] D. Kamburov, M. A. Mueed, M. Shayegan, L. N. Pfeiffer, K. W. West, K. W. Baldwin, J. J. D. Lee, and R. Winkler, Fermi contour anisotropy of GaAs electron-flux composite fermions in parallel magnetic fields, Phys. Rev. B **89**, 085304 (2014).

[39] Y. Liu, S. Hasdemir, L. N. Pfeiffer, K. W. West, K. W. Baldwin, and M. Shayegan, Observation of an Anisotropic Wigner Crystal, Phys. Rev. Lett. **117**, 106802 (2016).

[40] B. E. Feldman, M. T. Randeria, A. Gyenis, F. Wu, H. Ji, R. J. Cava, A. H. MacDonald, and A. Yazdani, Observation of a nematic quantum Hall liquid on the surface of bismuth, Science **354**, 316 (2016).

[41] I. Jo, K. A. Villegas Rosales, M. A. Mueed, L. N. Pfeiffer, K. W. West, K. W. Baldwin, R. Winkler, M. Padmanabhan, and M. Shayegan, Transference of Fermi contour anisotropy to composite fermions, Phys. Rev. Lett. **119**, 016402 (2017).

[42] Md. S. Hossain, M.K. Ma, Y. J. Chung, L. N. Pfeiffer, K. W. West, K. W. Baldwin, and M. Shayegan, Unconventional Anisotropic Even-Denominator Fractional Quantum Hall State in a System with Mass Anisotropy, Phys. Rev. Lett. **121**, 256601 (2018).

[43] M. S. Hossain, M. K. Ma, K. A. Villegas Rosales, Y. J. Chung, L. N. Pfeiffer, K. W. West, K. W. Baldwin, and M. Shayegan, Spontaneous valley polarization of itinerant electrons, Phys.

Rev. Lett. **127**, 116601 (2021).

[44] An anisotropic WS at high magnetic fields has been reported [39]. However, this state is observed under very specific and unusual conditions, namely in a 2D *hole* system confined to a wide GaAs quantum well, at a relatively large density and with a bilayer-like charge distribution, and only near the crossing of the lowest two Landau levels induced by tilting the sample in the magnetic field.

[45] T. Sajoto, Y. W. Suen, L. W. Engel, M. B. Santos, and M. Shayegan, Fractional quantum Hall effect in very-low-density GaAs/$Al_xGa_{1-x}As$ heterostructures, Phys. Rev. B **41**, 8449 (1990).

[46] J. Zhu, H. L. Stormer, L. N. Pfeiffer, K. W. Baldwin, and K. W. West, Spin susceptibility of an ultra-low-density two-dimensional electron system, Phys. Rev. Lett. **90**, 056805 (2003).

[47] M. Shayegan, E. P. De Poortere, O. Gunawan, Y. P. Shkolnikov, E. Tutuc, and K. Vakili, Two-dimensional electrons occupying multiple valleys in AlAs, Phys. Stat. Sol. (b) **243**, 3629 (2006).

[48] T. S. Lay, J. J. Heremans, Y. W. Suen, M. B. Santos, K. Hirakawa, M. Shayegan, and A. Zrenner, Highquality twodimensional electron system confined in an AlAs quantum well, Applied Physics Letters **62**, 3120 (1993).

[49] E. P. De Poortere, Y. P. Shkolnikov, E. Tutuc, S. J. Papadakis, and M. Shayegan, Enhanced electron mobility and high order fractional quantum Hall states in AlAs quantum wells, Appl. Phys. Lett. **80**, 1583 (2002).

[50] Y. J. Chung, K. A. Villegas Rosales, H. Deng, K. W. Baldwin, K. W. West, M. Shayegan, and L. N. Pfeiffer, Multivalley two-dimensional electron system in an AlAs quantum well with mobility exceeding 2×10^6 cm^2/Vs, Phys. Rev. Materials **2**, 071001(R) (2018).

[51] See Supplemental Material for a discussion on our material platform and additional data which includes Refs. [52–56].

[52] F. I. B. Williams, P. A. Wright, R. G. Clark, E. Y. Andrei, G. Deville, D. C. Glattli, O. Probst, B. Etienne, C. Dorin, C. T. Foxon, and J. J. Harris, Conduction Threshold and Pinning Frequency of Magnetically Induced Wigner Solid, Phys. Rev. Lett. **66**, 3285 (1991).

[53] E. M. Goldys, S. A. Brown, R. B. Dunford, A. G. Davies, R. Newbury, R. G. Clark, P. E. Simmonds, J. J. Harris, and C. T. Foxon, Magneto-optical probe of two-dimensional electron liquid and solid phases, Phys. Rev. B **46**, 7957 (1992).

[54] J. Zhao, Y. Zhang, and J. K. Jain, Crystallization in the fractional quantum Hall regime induced by Landau-level mixing, Phys. Rev. Lett. **121**, 116802 (2018).

[55] Kyung-Su Kim, Steven A. Kivelson, Discovery of an insulating ferromagnetic phase of electrons in two dimensions, Proc. National Acad. Sci. **118**, e2023964118 (2021).

[56] D. Shahar, D. C. Tsui, M. Shayegan, J. E. Cunningham, E. Shimshoni, S. L. Sondhi, On the nature of the Hall insulator. Solid State Commun. **102**, 817 (1997).

[57] To calculate r_s values, we use the effective in-plane band mass m^* which is equal to $(m_l m_t)^{1/2} = 0.46$. When electrons occupy a single valley, one can define r_s along [100] and [010] separately. This would lead to an anisotropic r_s. For example, when electrons occupy only the Y valley, $m_{[100]} = m_t = 0.2$ and $m_{[010]} = m_l = 1.1$. Therefore, $r_{s[010]} = 5.5 \times r_{s[100]}$. $r_{s[100]}$ and $r_{s[010]}$ are related to the r_s values that we used as follows: $r_s/0.46 = r_{s[100]}/0.2 = r_{s[010]}/1.1$.

[58] S. Ahn and S. D. Sarma, Valley polarization transition in a two-dimensional electron gas, arXiv:2110.09528 (2021).

[59] Note in Fig. 1(c) that near $n \simeq 2$, $R_{[100]}$ and $R_{[010]}$ show a second "kink" towards higher resistances at lower temperatures.

[60] Note that the power dissipated in the sample is much smaller than the cooling power of the cryostat. Also, Joule self-heating in the 2DES is not responsible for the nonlinearities we report: At a given density and temperature, the power required to achieve the same change in the differential resistance is more than an order of magnitude different along the two directions. We therefore conclude that the effect of heating is negligible in our measurements.

[61] S. T. Chui, Depinning, defect creation and quantum tunnelling, Phys. Lett. A **180**, 149 (1993).

[62] The parameter n_i is not precisely known for modulation-doped samples; it is typically smaller than the concentration of the δ-doping layer but larger than the 2DES density in the quantum well.

[63] H. Fukuyama and P. A. Lee, Dynamics of the charge-density wave. I. Impurity pinning in a single chain, Phys. Rev. B **17,** 535 (1978).

[64] L. Bonsall and A. A. Maradudin, Some static and dynamical properties of a two-dimensional Wigner crystal, Phys. Rev. B **15**, 1959 (1977).

[65] S. Das Sarma and E. H. Hwang, Low-density finite-temperature apparent insulating phase in two-dimensional semiconductor systems, Phys. Rev. B **68**, 195315 (2003).

[66] D. D. Vu and S. D. Sarma, Thermal melting of a quantum electron solid in the presence of strong disorder: Anderson versus Wigner, arXiv:2110.06229 (2021).

[67] B. I. Shklovskii, unpublished.